Saudi Journal of Biological Sciences 26 (2019) 2096–2101

Contents lists available at ScienceDirect

Saudi Journal of Biological Sciences

journal homepage: www.sciencedirect.com

Analysis of the protective mechanism of liraglutide on retinopathy based on diabetic mouse model

Lingling Wu [a], Lijuan Gao [b], Yaohui Cao [a,*], Fengju Chen [c], Ting Sun [a], Yahong Liu [d]

[a] Department of Gynaecology, Second Affiliated Hospital of Xingtai Medical College, Xingtai City 054000, China
[b] Department of Clinical Medicine, Xingtai Medical College, Xingtai City 054000, China
[c] Release Therapy Division, Second Affiliated Hospital of Xingtai Medical College, Xingtai City 054000, China
[d] Department of Endocrinology, Second Affiliated Hospital of Xingtai Medical College, Xingtai City 054000, China

ARTICLE INFO

Article history:
Received 29 August 2019
Revised 24 September 2019
Accepted 29 September 2019
Available online 16 October 2019

Keywords:
Diabetic retinopathy
Diabetes
Liraglutide
Retina
Mouse

ABSTRACT

In order to study the protection mechanism of liraglutide on the infectious lesion of the retina of type I diabetes, in this experiment, a mouse model of type I diabetes was established by induction with streptozotocin (STZ) and feeding with high-fat and high-sugar diet. After observing the living conditions of the modeled mice and detecting their fasting blood glucose (FBG), it was found that the modeled mice exhibited clinically similar symptoms in patients with type I diabetes, and their FBG was larger than 16.7 mmol/L, indicating that the experimental mouse model was obtained. The mice were divided into groups. The control group was divided into negative control group (A), light positive control group (B), diabetic control group (C), and diabetes care group (D) according to different treatment methods, and the experimental group was divided into treatment group 1 (LR1), treatment group 2 (LR2) and treatment group 3 (LR3) according to different injection doses. The eyes of mice in each group were extracted and retinal tissue sections were made, and the sections were stained with HE. The retinal morphology was observed and it was found that compared with group A, the outer nucleus layer was significantly thinner in group B and C, and the group D was the thinnest. After treatment with liraglutide, the outer nuclear layer of LR1 group and LR2 group LR3 group recovered significantly, indicating that liraglutide had protective effect on type I diabetes and light-induced damage of mouse retinal photoreceptor cells. Immunohistochemistry was used to detect p-Erk1/2 and ASK1 protein contents in retina. It was found that compared with the negative control group and the light control group, p-Erk1/2 protein contents in LR1, LR2 and LR3 groups were significantly increased, showing statistical significance. Compared with the negative control group and the light control group, ASK1 protein content in LR1, LR2 and LR3 groups significantly decreased. This suggested that the protective mechanism of liraglutide on retinopathy was related to up-regulation of antioxidant protein p-Erk1/2 and down-regulation of apoptosis-related protein ASK1, that is to say, the action site of liraglutide may be related to this. Through real-time quantitative detection of the Trx gene expression level in diabetic and photodamaged mice, it was found that compared with the diabetic light group, the Trx expression level in mice treated with liraglutide showed a significant up-regulated trend, suggesting that the protective mechanism of liraglutide on retinopathy was related to the up-regulated expression of antioxidant protein Trx. Therefore, liraglutide has a certain protective effect on diabetic retinal injury, and its mechanism is related to the up-regulation of p-Erk1/2 and Trx antioxidant protein, and the down-regulation of apoptosis-related protein ASK1.

© 2019 Production and hosting by Elsevier B.V. on behalf of King Saud University. This is an open access article under the CC BY-NC-ND license (http://creativecommons.org/licenses/by-nc-nd/4.0/).

1. Introduction

Diabetes is a metabolic disease characterized by hyperglycemia caused by insufficient insulin secretion or its blocked biological mechanism, or both (Zhang et al., 2017a,b). Diabetes can be divided into type I diabetes and type II diabetes, both of which have significant genetic heterogeneity and a family-borne tendency. With the improvement of people's living standards, the dietary structure of

* Corresponding author.
E-mail address: cao.yaohui@yahoo.com (Y. Cao).

Peer review under responsibility of King Saud University.

Production and hosting by Elsevier

https://doi.org/10.1016/j.sjbs.2019.09.032
1319-562X/© 2019 Production and hosting by Elsevier B.V. on behalf of King Saud University.
This is an open access article under the CC BY-NC-ND license (http://creativecommons.org/licenses/by-nc-nd/4.0/).

human beings has changed, and the diet with high sugar, fat and calories is the main reason for the rapid increase of diabetes incidence (Li et al., 2017). However, if the blood glucose level in the body can't be reduced to the normal level for a long time, it will lead to chronic damage or dysfunction of eyes, kidneys, heart, blood vessels and nerves in particular (Bugáňová et al., 2017).

The most common complication of diabetes is the Diabetic Retinopathy (DR) of the patient. DR is a specific fundus change with complicated pathogenesis, which can lead to blindness if untreated (Von Scholten et al., 2017). Nowadays, diabetic retinopathy has become the main cause of acquired blinding eye disease. In clinical practice, diabetic retinopathy is usually classified into proliferative diabetic retinopathy and non-proliferative diabetic retinopathy according to the presence of retinal neovascularization (Babateen et al., 2017). The pathogenesis of retina is complex, which is mainly believed to be related to the abnormal metabolism of polyol and inositol, the imbalance of free radicals, oxidation and reduction potential energy, inositol depletion, cytokines and other factors (Liou et al., 2018).

At present, there are two theories that can explain the pathogenesis of diabetic retinopathy, namely the theory of retinal microangiopathy and the theory of retinal neuropathy. According to the theory of retinal microangiopathy, long-term exposure to hyperglycemia results in dysfunction of retinal vascular endothelial function, which leads to retinal microvascular injury and microangiopathy (Wang, 2018). Some studies have found that long-term increase of blood glucose will produce too many reactive oxygen molecules, which can't be cleared by the body in time. Therefore, proteins, oxidized cell membranes and unsaturated fatty acids in the cytoplasm are saccharified. This toxic effect on the body tissue is vascular endothelial cells, which is the main cause of microvascular injury in diabetes, and then leads to retinopathy. According to the theory of retinal neuropathy, hyperglycemia will cause changes in endothelial cells, lead to vascular stenosis, reduce blood flow, cause ischemia and hypoxia of ocular nerve network tissue, hinder tissue energy metabolism, and finally cause retinal diseases (Zhang et al., 2018).

Glucagon-like peptide-1 (GLP-1) is an incretin synthesized and secreted by intestinal L cells, which is distributed as a site in human retina, nervous system and pancreatic tissues (Bruen et al., 2017). Liraglutide is a GLP-1 analogue developed by Novo Nordisk in Denmark and is used clinically to control blood glucose levels in patients with type II diabetes. Some studies have found that liraglutide has protective effects on β cells and cardiovascular diseases, but the effect of liraglutide on retinopathy has been rarely studied (Zhang et al., 2017a,b). Based on the above understanding, in this research, a diabetic mouse model was established to study the mechanism of liraglutide in DR from the perspectives of histomorphology, protein expression level, and gene expression level.

2. Materials and methods

2.1. Selection and grouping of experimental animals

Forty healthy female Kunming mice of SPF grade were selected (provided by XX experimental animal center). The mice were required to be about 5 weeks old and weigh about 30 g. Feeding conditions of mice: constant temperature of 23 ± 2 °C, relative humidity of 60 ± 10%, alternating light of 12 h, the activity of cage feeding in mice was not limited, and the diet could be freely used. In addition, the eyeball of mice should be observed to make sure that the refractive medium of the eye was clear and no abnormality was found in the fundus. Experimental grouping method is shown in Table 1.

Table 1
Grouping table of diabetic mouse model.

	No.	Name	Quantity (case)
Control group	A	Negative control group	5
	B	Light positive control group	5
	C	Diabetes control group	5
	D	Diabetes Light Group	5
Experimental group	LR1	Treatment group 1	5
	LR2	Treatment group 2	5
	LR3	Treatment group 3	5

2.2. Method for establishing diabetes mouse model

Experimental group: thirty mice were randomly selected (five of which were used to supplement the mice that failed in modeling), and the mice were first raised adaptively in the animal house with normal diet for one week. Then SD mice were fed with a high-fat and high-sugar diet (74.5% normal diet +10% lard +10% sugar +5% yolk powder +0.5% cholesterol) sterilized by ultraviolet radiation. After 2 weeks of continuous feeding, all mice fasted overnight (12 h), and the weight of each mouse was measured and recorded. STZ, which was prepared with 0.1 mol/L sterile citric acid buffer (pH = 4.4), was intraperitoneally injected into mice to induce diabetes at a dose of 85 mg/kg. It was injected once every five days for a total of two injections. After three days of the second injection, the tail tip of the mouse was subtracted from 1 to 2 mm, and the tail blood of the mouse was collected to measure FBG. When the amount of water, food intake and urine of the mice increased, and the FBG was greater than 16.7 mmol/L, the diabetic mouse model was successfully established. The successfully modeled diabetic mice were fed with high-fat and high-sugar diet for 2 weeks. Tail tip blood of the mice was collected every week to measure FBG, and the mice with high blood glucose (FBG > 16.7 mmol/L) were screened.

Control group: group A and group B were injected with the same amount of sterile citric acid buffer. Among them, illumination group and diabetic illumination group were illuminated for 72 h after administration.

2.3. Establishment of drug intervention model

In this study, mice were intraperitoneally injected with different doses of liraglutide (Novo Nordisk, Denmark). The doses of LR1, LR2 and LR3 groups were 62.5 g/kg, 175 g/kg and 250 mg/kg, respectively, according to the body weight of rats. Note that administration was given for a specific period of time each day, such as nine o'clock in the morning, for 10 consecutive days. The other control groups were intraperitoneally injected with the same dose of normal saline at the same time period.

2.4. Treatment methods of retinal tissue sections

After the mice were sacrificed by cervical dislocation, the eyeballs were quickly removed and were marked at 12: 00. Both eyes were fixed in 10% neutral formalin fixator for 24 h, and 70% alcohol was transferred for 48 h. Then, 80%, 95% and 100% alcohol were added twice, each time for 30 min. After each step dehydration, xylene was used for transparency for 4 times, each time for 15 min. The transparent tissue blocks were placed in liquid paraffin wax and placed in a wax melting box at 58 °C overnight. The next day, paraffin wax was replaced and the sample was continued to be soaked in wax for 4 h before embedding. Finally, the wax blocks were stored in a refrigerator at 4 °C.

2.5. HE staining method

Sagittal section was made along the optic nerve at 12:00 of the eyeball, and the section had a thickness of 5 μm. The slice was spread in a water bath box at 49 °C and pasted on a glass slide coated with polylysine. It was baked at 42 °C for 48–72 h in a constant temperature box for later use. The glass slides were dewaxed with toluene for 2 times, each time for 10 min. The water was dehydrated by 100%, 90% and 80% gradient ethanol for 3 min, respectively. The sample was washed with distilled water for 3–5 min and then stained with hematoxylin for 10 min. It was then washed with distilled water for 3 min, followed by 1% hydrochloric acid alcohol for color separation, and then washed with distilled water for anti-blue for 30 min. It was stained with eosin for 5 min and then washed with distilled water for 10 min. The samples were dehydrated with 80% ethanol for 1 min and 90% ethanol for 1 min. Xylene was used to make the slices transparent, and seal them with neutral gum. Finally, HE staining was completed.

Changes in the thickness of photoreceptor nuclear layer in the retina were observed under an optical microscope (Olympus, Japan), the number of layers of the outer nuclear layer of the retinal photoreceptor was counted and counted, so as to analyze the relationship between the amount of 6 doses and the degree of retinal damage.

2.6. Method for detecting p-Erk1/2 and ASK1 by immunohistochemistry

Firstly, the above paraffin sections were subjected to conventional dewaxing: the sample was dewaxed twice with xylene for 20 min each time. It was dehydrated with 75%, 90% and 100% ethanol for 3 min at a time. Finally, it was gently rinsed 3 times with distilled water for 3 min each time;

Secondly, inactivation by endogenous enzyme: 3% hydrogen peroxide and distilled water were mixed at a ratio of 1:10, and the slices were immersed in the mixture at room temperature for 5–10 min to inactivate the endogenous enzyme, then it was washed three times with distilled water for 5 min each time.

Thirdly, microwave heat was used to repair antigens: the sections were immersed in citrate buffer (pH 6.0), and the microwave oven was set to mid-range and the sample was heated to boiling and then removed. After standing for 5–10 min at room temperature, the microwave oven was adjusted to the middle and low range, and the sample was heated again for 5 min, and took out to cool at room temperature. Be careful not to shake the beaker vigorously during the whole process, or it would easily lead to peeling. After cooling, it was washed 3 times with PBS buffer of pH 7.0 for 5 min each time.

Fourthly, seal: normal goat serum blocking solution was added dropwise, and the excess liquid was removed at room temperature for 30 min.

Fifthly, drop the primary antibody: the antibodies of p-Erk1/2 and ASK1 were diluted with antibody diluent at the ratio of 1:200, and then the diluted antibodies were added to the sections respectively, and incubated at 37 °C for 2 h at a constant temperature. It was washed 3 times with PBS buffer for 3 min each time.

Sixthly, drop the second antibody: Polymer helper was added, the sample was incubated for 20 min at 37 °C, washed with PBS for 3 times, each time for 3 min. Then, Poly peroxidase-anti-mouse (IgG) was added and incubated at 37 °C for 20 min. The sample was washed 3 times with PBS buffer for 3 min each time.

Seventh, DAB color development: the PBS buffer was dried, 1 drop of reagents A, B and C in DAB reagent kit were added into 1 mL distilled water and mixed evenly. The mixed liquid was dropped into slices and observed under microscope at room temperature to control color rendering. When more brown-yellow products appeared, the chromogenic reaction was terminated.

Eighthly, the sample was slowly buffered with distilled water, mildly counterstained with a small amount of hematoxylin, and differentiated with hydrochloric acid alcohol.

Ninthly, the slices were dehydrated with 75%, 90% and 100% ethanol, transparent by xylene and sealed with neutral gum.

Tenthly, the samples were observed under a microscope, and the average optical density values of the immunohistochemical stained sections were measured and statistically analyzed with the image processing software lmage-Pro Plus 6.0.

2.7. Method for extracting mRNA of retinal Trx gene

Firstly, the mice were sacrificed by CO_2 inhalation method, the eyeballs were immediately removed and placed on ice, and the retina was peeled off under an inverted microscope (Olympus, Japan). Secondly, 1 mL of Trizol was added to the retinal tissue of the mouse (from two eyeballs), homogenized on an ice with an ultrasonic pulverizer for about 20 s; and allowed to stand at room temperature for 15 min. Thirdly, it was centrifuged at 4 °C and 12000 rpm for 5 min in a cryogenic freezing centrifuge (Beijing Tetraloop Scientific Instrument Factory, China). The supernatant was carefully absorbed and transferred into a new centrifuge tube, paying attention not to absorb the sediment. Fourthly, chloroform was added to the supernatant according to a dose of 1:5 (200 μL of chloroform per mL sample), and the mixture was shaken vigorously and allowed to stand at room temperature for 10 min. Fifthly, the samples were centrifuged in a cryogenic centrifuge at 4 °C and 12000 rpm for 15 min, and the supernatant was carefully transferred to a new centrifuge tube. Sixthly, 2.5 X absolute ethanol was added to the supernatant, gently shaken and mixed, and allowed to stand at −20 °C for 30 min. Seventhly, the samples were centrifuged in a cryogenic centrifuge at 4 °C and 12000 rpm for 10 min, the supernatant was discarded, and 250 μL 75% DEPC-ethanol was added to the precipitation, and gently oscillated and suspended. Eighthly, the samples were centrifuged in a cryogenic centrifuge at 4 °C and 12000 rpm for 5 min, and then the supernatant was lightly discarded. The EP tube was opened and placed upside down on the absorbent paper for 2–5 min at room temperature. Ninthly, RNase-free of 20 μL was added, and the precipitate was lightly blown with pipet gun or put into a 37 °C water bath box (Jiangsu Quantan Instrument Factory, China) to dissolve the RNA. Note that plastic instruments such as EP tubes should be treated by 0.1% DEPC (PIERCE, USA), and glass instruments should be sterilized by high temperature and high pressure to remove RNase, and the cryogenic centrifuge should be precooled at 4 °C before the experiment.

2.8. Real time PCR method

First, reverse transcription of Trx gene RNA to synthesize cDNA.

After the RNA precipitate was completely dissolved, the concentration was measured with a microplate reader (Thermo Scientific, USA). In each experimental group, 1 μL LRNA was used for reverse transcription to prepare cDNA, and the reverse transcription kit (Beijing Qingke Xinye Biotechnology Co., Ltd.) was used for operation. The reaction system is shown in Table 2. The reverse transcription reaction conditions were 50 °C for 30 min; 99 °C for 5 min; and 5 °C for 5 min.

Second, real time PCR.

Primer design: mRNA sequences of Trx genes were searched in Genbank, and Primer Premier5.0 was used to design primers in a reading frame. Primer sequences (Synthesized by Beijing Qingke Xinye Biotechnology Co., Ltd.) are shown in Table 3.

Table 2
Reverse transcriptional reaction system.

MgC2	1 μL
10XRT Buffer	1 μL
RNase Free dH20	3.75 μL
dNTP Mixture	1 μL
RNase Inhibitor	0.25 μL
AMV Reverse Transcriptase	0.5 μL
Oligo dT-Adaptor Primer	0.5 μL
RNA	1 μL
Total	10 μL

Table 3
Trx gene primer sequences.

Gene name	Primer sequence	
Trx	F	GGAATGGTGAAGCAGATCGAG
	R	ACGCTTAGACTAATTCATTAAT
GAPDH	F	TGTGATGGGTGTGAACCACGAGAA
	R	GAGCCCTTCCACAATGCCAAAGTT

Real time PCR was performed by using the real time PCR kit (Dalian TaKaRa Co., Ltd.), taking the cDNA of Trx gene as the template, and adding other components of PCR. The PCR products were subjected to agarose gel electrophoresis, observed under ultraviolet lamp, imaged with GIS gel imaging system, and semi-quantitatively analyzed to detect the expression level of Trx.

PCR reaction conditions: 94 °C (2 min); 94 °C (30 sec); 56 °C (30 sec); 72 °C (15 sec); 72 °C (10 min). All the cases were repeated for 27–30 cycles (see Table 4).

2.9. Statistical method

SPSS21.0 was used in this experiment, mean ± standard deviation was used to represent the experimental data, and *t*-test was used for mean comparison. One-way ANOVA was used to analyze the difference, and the difference was statistically significant when $P < 0.05$.

3. Results

3.1. Diabetic rat modeling results

Through observation, it was found that the weight of the rats in the control group (group A and group B) increased with the increase of week age, the hair was bright and smooth, the growth and mental state were good, the action was agile, the FBG was maintained between 3.0 and 5.0 mmol/L, and the amount of water and urine was the same as before. Compared with the control group, the diabetic modeling rats showed disorderly fur, listlessness, inactivity and irritability, significantly increased food intake, water intake and urine volume, and significantly decreased body weight with the increase of week age (as shown in Table 5). They showed the symptoms of typical diabetes, namely "more drinking, more urine, more food and less weight". The measurement results

Table 4
Real time PCR reaction system.

5 × PCR Buffer	10 μL
Sterilized distilled water	28.75 μL
TakaRa Ex Taq HS	0.25 μL
Upstream specific primer	0.5 μL
Downstream specific primer	0.5 μL
Tatal	40 μL

Table 5
Body weight results of each group of mice (g).

Groups	One week after STZ injection	Two weeks after STZ injection
Blank control group	251.19 ± 18.21	366.58 ± 32.05
Diabetes model group	156.22 ± 8.14*	130.04 ± 7.58*

* $P < 0.05$ vs Blank control group.

Table 6
FBG results (mmol/L) in each group of mice.

Groups	One week after STZ injection	Two weeks after STZ injection
Blank control group	3.95 ± 0.60	3.63 ± 0.33
Diabetes model group	21.04 ± 3.11*	21.35 ± 3.58*

* $P < 0.05$ vs Blank control group.

of FBG of mice in each group are shown in Table 6. Compared with the blank control group, FBG of mice in the diabetes group was greater than 16.7 mmol/L, and FBG was significantly increased ($P < 0.01$), which was statistically significant, indicating the successful model of STZ-induced diabetes mice.

3.2. Statistical results of the retinal photoreceptor nuclear layer

Morphological observation of the retinal sections after HE staining and measurement of the thickness of the outer nuclear layer (Figs. 1 and 2) revealed the following results: firstly, the negative control group (group A) had uniform staining, clear tissue structure and orderly cell arrangement. Secondly, compared with the negative control group (13.58 ± 1.49), the positive control group (group B and group C) had significantly thinner outer nuclear layer, significantly sparse retinal cell arrangement, and significantly disordered, swollen and broken arrangement of inner and outer nodes. Thirdly, when diabetic mice were exposed to strong light, the outer nuclear layer thickness of group D mice was (7.60 ± 1.31), which was significantly reduced compared with group A ($P < 0.001$). Fourthly, compared with group C (9.47 ± 0.61), the outer nuclear layer of group D was further thinner and the retinopathy was more serious. Fifthly, the retinal structure of the liraglutide treatment group (LR1 group, LR2 group, LR3 group) was better than that of the positive control group, with slightly sparse arrangement of retinal cells, slightly disordered

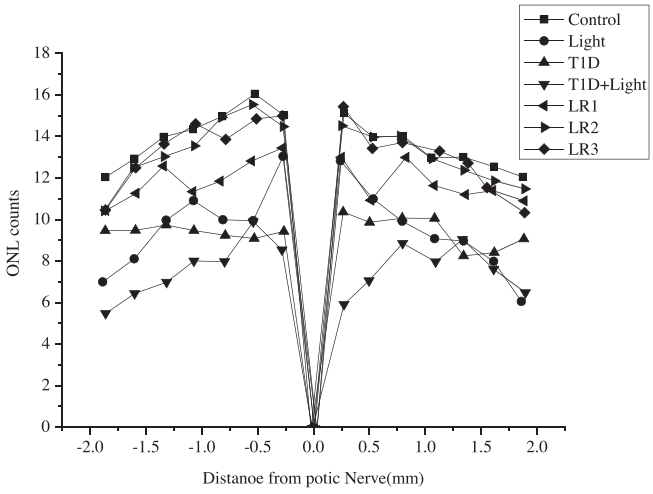

Fig. 1. Count statistics of outer core layer.

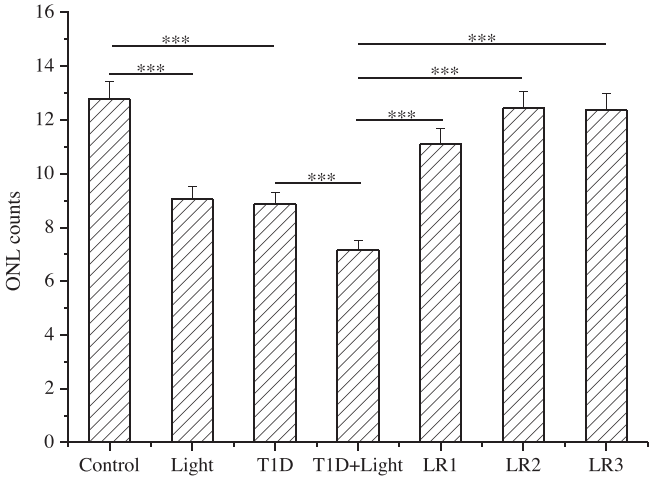

Fig. 2. Statistical chart of measurement results of outer core layer thickness.

arrangement of inner and outer segments, swelling, fragmentation, and slightly thinning of outer nuclear layer. Compared with group C, the thickness of outer nuclear layer in the treatment group was 11.92 ± 0.91, 13.38 ± 1.52, 13.63 ± 1.69, which were significantly increased ($P < 0.001$).

Therefore, it can be explained that liraglutide protects against damage of mouse retinal photoreceptor cells induced by type I diabetes and light.

3.3. Results of p-Erk1/2 detected by immunohistochemistry

The average optical density value of p-Erk1/2 immunohistochemical staining sections of mouse retina was measured. The statistical results are shown in Fig. 3. It was found that the expression of p-Erk1/2 in the group B (1.45 ± 0.007) was significantly reduced compared with the group A (2.30 ± 0.004). Compared with group A (2.30 ± 0.004), the expression levels of p-Erk1/2 in group LR1, LR2 and LR3 were 2.14 ± 0.014, 2.12 ± 0.018 and 3.16 ± 0.021, respectively, and the expression levels were significantly increased ($p < 0.001$). Therefore, it was suggested that liraglutide could up-regulate the expression of p-Erk1/2, and the protective mechanism of liraglutide on retinopathy was related to the up-regulated expression of antioxidant protein p-Erk1/2.

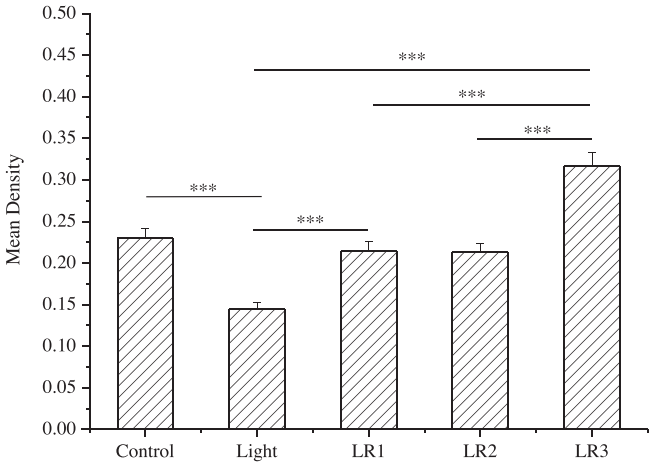

Fig. 3. Results of p-Erk1/2 expression in the retina by immunohistochemistry.

3.4. Results of ASK1 detected by immunohistochemistry

The average optical density value of ASK1immunohistochemical staining sections of retina in mice was measured. The statistical results are shown in Fig. 4. It was found that compared with the negative control group (0.22 ± 0.024), the ASK1 expression level in the light group (0.33 ± 0.013) increased significantly ($P < 0.01$), and the difference was statistically significant. Compared with the light group (0.33 ± 0.013), ASK1 expression levels in LR 1 group (0.20 ± 0.003, $P < 0.001$), LRI2 group (0.24 ± 0.009, $P < 0.01$) and LRII3 group (0.20 ± 0.003, $P < 0.001$) were all significantly down-regulated. Therefore, it was suggested that liraglutide could down-regulate the expression of ASK1, and the protective mechanism of liraglutide on retinopathy was related to down-regulation the expression of apoptosis-related protein ASK1.

3.5. Test results of real-time PCR

The following results were obtained by real-time quantitative analysis of the expression levels of Trx gene in diabetic and photodamaged mice, as shown in Fig. 5. Firstly, the expression level of Trx gene in diabetic and photodamaged mice was downregulated. Compared with the negative control group (0.698 ± 0.11), the Trx gene expression level in the diabetic control group (0.60 ± 0.06)

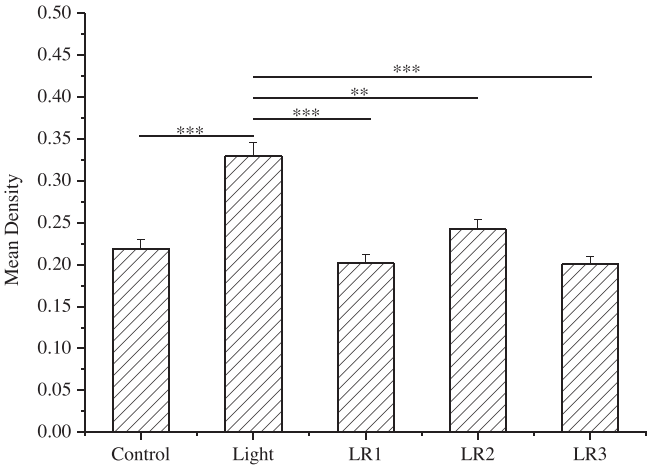

Fig. 4. Results of ASK1 expression in the retina by immunohistochemistry.

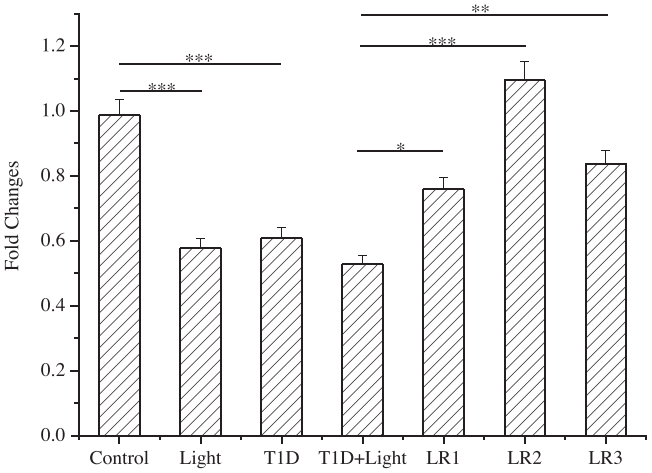

Fig. 5. Real time PCR of Trx.

and the light group (0.57 ± 0.05) was significantly reduced ($P < 0.01$), and the difference was statistically significant. Second, Trx expression in the diabetic light group (0.53 ± 0.08) was significantly lower than that in the diabetic control group ($P < 0.05$). Compared with the diabetic light group, the expression of Trx was significantly up-regulated in LR 1 group (0.76 ± 0.13, $P < 0.05$), LR 2 (1.09 ± 0.09, $P < 0.001$) and LR 3 (0.84 ± 0.11, $P < 0.01$). Therefore, it was suggested that liraglutide could up-regulate the expression of Trx, and the protective mechanism of liraglutide on retinopathy was related to the up-regulated expression of antioxidant protein Trx.

4. Discussion

The pathological process of diabetic retinopathy is very complicated, and its occurrence involves many factors. In recent years, some scholars have proposed that its etiology is related to oxidative stress (Chen et al., 2017). It is believed that due to the long-term increase of blood glucose level in the body, the body produces excessive reactive oxygen radicals that can't be cleared, which can oxidize the cell membrane, namely unsaturated fatty acids, saccharify proteins, damage the DNA structure, and poison the body tissues. The clinical manifestations of this toxic effect in the eyes are increased retinal oxidative damage and sensory cell apoptosis (Kowluru and Shan, 2017). In this experiment, a mouse model of type I diabetes was established by intraperitoneal injection of STZ in Kunming mice to induce diabetes and feeding with high-fat and high-sugar diet. By observing the retinal tissue of each group of mice, it was found that the outer nuclear layer of the diabetic light group was the thinnest and the damage was the most serious. After treatment with liraglutide, the outer nuclear layer of LR1, LR2, and LR3 groups recovered significantly, indicating that liraglutide had protective effects on type I diabetes and light-induced photoreceptor cells in mice. Immunohistochemistry was used to detect p-Erk1/2 and ASK1 protein contents in the retina. And it was found that compared with the negative control group and the light control group, p-Erk1/2 protein contents in LR1, LR2 and LR3 groups were significantly increased. Compared with the negative control group and the light control group, ASK1 protein content in LR1, LR2 and LR3 groups was significantly reduced, suggesting that the protective mechanism of liraglutide on retinopathy was related to up-regulation of antioxidant protein p-Erk1/2 and down-regulation of apoptosis-related protein ASK1. By detecting the expression level of Trx gene, it was found that the expression level of Trx in mice treated with liraglutide showed a significant up-regulation trend, suggesting that liraglutide may achieve therapeutic effect by up-regulating the antioxidant protein Trx. The results of this study are consistent with the above oxidative stress theory.

In summary, liraglutide reduced oxidative damage by up-regulating the expression of the oxidation-related proteins p-Erk1/2 and Trx and down-regulating the expression of the apoptosis-related protein ASK1, thereby achieving the control of retinal damage caused by type I diabetes and photodamage. However, this result can't specifically explain the specific action site of liraglutide in DR therapy, so further research on this pathway is needed. In addition, the drug gradient of liraglutide set in this experiment has no obvious effect on retinal treatment, which can't explain the relationship between drug dosage and DR treatment, so further research is needed.

References

Babateen, O., Korol, S.V., Jin, Z., 2017. Liraglutide modulates GABAergic signaling in rat hippocampal CA3 pyramidal neurons predominantly by presynaptic mechanism. Bmc Pharmacol. Toxicol. 18 (1), 83–85.

Bruen, R., Curley, S., Kajani, S., 2017. Liraglutide dictates macrophage phenotype in apolipoprotein E null mice during early atherosclerosis. Cardiovasc. Diabetology 16 (1), 143–147.

Bugáňová, M., Pelantová, Helena, Holubová, Martina, 2017. The effects of liraglutide in mice with diet-induced obesity studied by metabolomics. J. Endocrinol. 233 (1), 93–96.

Chen, X., Wu, R., Kong, Y., 2017. Tanshinone II Aattenuates renal damage in STZ-induced diabetic rats via inhibiting oxidative stress and inflammation. Oncotarget 8 (19), 31915–31922.

Kowluru, R.A., Shan, Y., 2017. Erratum to: Role of oxidative stress in epigenetic modification of MMP-9 promoter in the development of diabetic retinopathy. Graefes Arch. Clin. Exp. Ophthalmol. 255 (5), 1055–1056.

Li, J., Fu, L.Z., Liu, L., 2017. Glucagon-like peptide-1 (GLP-1) receptor agonist liraglutide alters bone marrow exosome-mediated miRNA signal pathways in ovariectomized rats with type 2 diabetes. Med. Sci. Monitor Int. Med. J. Exp. Clin. Res. 23, 5410–5419.

Liou, J.H., Liu, Y.M., Chen, C.H., 2018. Management of diabetes mellitus with glucagonlike peptide-1 agonist liraglutide in renal transplant recipients: a retrospective study. Transpl. Proc. 50 (8), 2502–2505.

Von Scholten, Bernt J., Persson, F., Rosenlund, S., 2017. The effect of liraglutide on renal function: A randomized clinical trial. Diabetes Obes. Metab. 19 (2), 239–244.

Wang, P., 2018. Long term application of Liraglutide on carotid atheromatous plaque reversal in patients with type 2 diabetes. China Med. Abstr. (Intern. Med.) 35 (1), 22–23.

Zhang, Y., Ling, Y.N., Yang, L., 2017a. Liraglutide relieves myocardial damage by promoting autophagy via AMPK-mTOR signaling pathway in zucker diabetic fatty rat. Mol. Cell. Endocrinol. 448 (23), 98–103.

Zhang, L., Zhang, S.T., Yin, Y.C., 2018. Hypoglycemic effect and mechanism of isoquercitrin as an inhibitor of dipeptidyl peptidase-4 in type 2 diabetic mice. RSC Adv. 8 (27), 14967–14974.

Zhang, Y., Zhao, H., Li, H., 2017b. Protective effects of amarogentin against carbon tetrachloride-induced liver fibrosis in mice. Molecules 22 (5), 754–758.